Tidal amplification and river capture in response to land reclamation in the Ganges-Brahmaputra delta

van Maren, D. S.; Beemster, J. G.W.; Wang, Z. B.; Khan, Z. H.; Schrijvershof, R. A.; Hoitink, A. J.F.

DOI
10.1016/j.catena.2022.106651

Publication date
2023

Document Version
Final published version

Published in
Catena

Catena 220 (2023) 106651

Contents lists available at ScienceDirect

Catena

journal homepage: www.elsevier.com/locate/catena

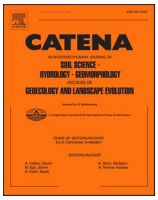

Tidal amplification and river capture in response to land reclamation in the Ganges-Brahmaputra delta

D.S. van Maren [a,b,c,*], J.G.W. Beemster [d], Z.B. Wang [b,c], Z.H. Khan [e], R.A Schrijvershof [c,d], A.J.F. Hoitink [d]

[a] State Key Lab of Estuarine and Coastal Research, East China Normal University, Shanghai 200241, China
[b] Faculty of Civil Engineering and Geosciences, Delft University of Technology, Delft 2600GA, The Netherlands
[c] Deltares, Marine and Coastal Systems Unit, Boussinesqweg 1, 2629 HV Delft, The Netherlands
[d] Department of Environmental Sciences, Wageningen University and Research, Wageningen, The Netherlands
[e] Institute of Water Modelling (IWM), House 06, Road 3C, Block H, Sector 15, Uttara, Dhaka 1230, Bangladesh

ARTICLE INFO

Keywords:
Ganges-Brahmaputra delta
Tidal amplification
Estuary
Fine sediments
Land reclamations
Human impacts

ABSTRACT

At a global scale, intertidal areas are being reclaimed for agriculture as well as urban expansion, imposing high human pressure on the coastal zone. The Ganges-Brahmaputra Delta (GBD) is an exponent of this development. In this delta, land reclamation accelerated in the 1960's to 1980's, when polders were constructed in areas subject to regular marine flooding. A comprehensive analysis of tidal channel evolution in the southwest GBD reveals how land reclamation leads to tidal amplification, channel shoaling, bank erosion, and interaction between channels in which one tidal river captures the storage area of a neighbouring river. We identify-two positive feedback mechanisms that govern these morphological changes. First, reclaiming intertidal areas results in immediate loss of tidal storage, which leads to amplification and faster propagation of the tides. In systems with abundant sediment supply, the blind tidal channels progressively fill in with sediment, leading to a continued loss of tidal storage and therefore further distorting the tides. Secondly, when intertidal areas of parallel (and inter-connected) river delta distributaries are asynchronously or unevenly reclaimed, one channel distributary may expand its intertidal area at the expense of the other. This is initiated by an increasing propagation speed of the tidal wave in the partially reclaimed distributary, travelling into the non-reclaimed distributary through connecting channels. These connecting channels progressively expand while the pristine channel shoals, and potentially degenerates. Both positive feedback loops are very stable and are responsible for pluvial flooding of polders, large-scale bank erosion, and poorly navigable primary waterways, including the navigation channel accessing Bangladesh's second-largest port. Interventions aiming to solve these problems have to account for the complex positive feedback mechanisms identified in this paper and be nature-based and holistic.

1. Introduction

River deltas result from the interaction between fluvial sediment supply and subsequent remolding and dispersion of sediment by waves and tides (Wright and Coleman, 1973). Deltas are under pressure for a number of reasons related to human interventions and climate change. The largest threat is the change in sediment flux (Ericson et al., 2006), which may increase due to deforestation (e.g. Nienhuis et al., 2020) or decrease due to trapping of sediment in reservoirs (Vörösmarty et al., 2003; Syvitski et al., 2005). Even in the past 30 years, despite building of reservoirs, deltas still experience net land growth, partly resulting from deforestation (Nienhuis et al., 2020). Another major challenge to deltas is relative sea level rise, either through local subsidence resulting from groundwater extraction (Syvitski et al., 2009), or eustatic sea level rise (Nicholls and Cazenave, 2010; Bilskie et al., 2014). A third major threat is urbanization (Renaud et al., 2013) resulting in less sediment trapping on the delta plain (Giosan et al., 2014) and strongly modified hydrodynamics (Winterwerp and Wang, 2013; Talke and Jay, 2020). River deltas form a complex network of channel distributaries, which are increasingly modulated by tides in the seaward direction. Such a

* Corresponding author at: State Key Lab of Estuarine and Coastal Research, East China Normal University, Shanghai 200241, China.
E-mail address: bas.vanmaren@deltares.nl (D.S. van Maren).

https://doi.org/10.1016/j.catena.2022.106651
Received 7 March 2022; Received in revised form 8 July 2022; Accepted 16 September 2022
Available online 1 October 2022

complex tidal network forms a delicate morphodynamic equilibrium, albeit more stable than their fluvial counterparts – Hoitink et al. (2017); Lentsch et al., (2018); Iwantoro et al. (2020). A perturbation to this balance may result in a large-scale network reorganization (Fagherazzi, 2008; Bain et al., 2019). Channel networks are therefore sensitive to human interventions.

An example of a delta under great anthropogenic threat at various spatial scales is the Ganges-Brahmaputra Delta (hereafter referred to as the GBD). The GBD is one of the most vulnerable deltas of the world (Syvitski et al., 2009; Tessler et al., 2015; Passalacqua et al., 2021) and is affected by extreme events, climate change and human interventions. The low-lying delta is prone to fluvial, coastal, and pluvial flooding, resulting from high rainfall in combination with poor drainage. Often, various types of flooding occur simultaneously. Catastrophic high river floods may inundate up to 50 % of the country (1998 flood; Chowdhury, 2000) while at the same time, Bangladesh is highly susceptible to tropical cyclones (Islam and Peterson, 2009). Bhola, the deadliest cyclone in human history, claimed more than 250.000 casualties in 1970 (Hossain, 2018). Mean sea levels are gradually increasing because of eustatic sea level rise (3 mm/y; Pethick and Orford, 2013) and subsidence (2.9 mm/y on average; Brown and Nicholls, 2015). The GBD is also the world's most populous delta with 170 million inhabitants (Paszkowski et al., 2021), resulting in large potential loss of life and livelihood during flooding, but also in pronounced human interventions in the delta system. These anthropogenic disturbances may aggravate the impacts of extreme events and sea level rise, and can drive endogenous morphologic developments in the delta that may overwhelm the anticipated risks associated with climate change (Paszkowski et al., 2021). For instance, the construction of polders in the southwest GBD is the main factor controlling bed levels (Auerbach et al., 2015), river infilling (Wilson et al., 2017) and increasing high waters (rising with 15–17 mm/y; Pethick and Orford, 2013), resulting in higher levels of geomorphic change in the embanked section of the delta compared to the more pristine Sundarbans mangrove forest (Jarriel et al., 2020).

Since the 1960's, 5000 km^2 of intertidal and supratidal land was converted into densely populated polders (Wilson et al., 2017). The channels draining these reclaimed areas filled up with sediments as a result of a sharp reduction of the flow velocity. Over 1000 km of such channels were impacted by polder construction and their subsequent infilling resulted in the creation of 90 km^2 new land. More than 400 km of the primary waterways lost over 50 % of their original width (Wilson et al., 2017). Infilling of the channels leads to a progressive reduction in tidal prism, therefore of the tidal flow velocities, which leads to subsequent infilling in the seaward direction. This self-reinforcing process leads to progressive infilling of the delta plain, and in the recent past, 16 km of channels still close every year (Wilson et al., 2017). In the southwest GBD, Bain et al. (2019) observed that the loss in tidal prism resulted in tidal channel distributaries competing for the available tidal prism through expansion of smaller river systems connecting the main distributaries. This leads to an increase in the tidal discharge in one channel at the expense of another, controlling infilling of the degenerating tidal channel and widening of the other main channel and the channels connecting them.

Summarizing, the work of Pethick and Orford (2013) shows that the tidal range is amplifying (likely also in response to polder construction), Wilson et al. (2017) describe how dead-end channels are rapidly filling in, and Bain et al. (2019) followed up on this by demonstrating that the channel network reorganizes in response to polder construction (resulting in expanding connecting channels and shoaling of a degenerating tidal branch). These key papers have significantly advanced our understanding of the dynamic behaviour of tidal channels in delta networks, particularly in the southwest GBD. The aim of this paper is to advance on these previous studies by developing a conceptual framework explaining how polder construction influenced tidal amplification, channel degeneration, and network reorganisation. We argue that this behaviour is controlled by two very stable positive feedback mechanisms continuously reshaping the delta, 60 years after the initial construction of polders. For this purpose, we analyse tide gauge data and coastline changes (based on a map and satellite imagery), each covering an observational period of 80 years, and bathymetric data since the 1970's, which we analyse and explain using numerical models.

The structure of this paper is as follows. We first quantify observed changes of water levels through analysis of existing water level gauges dating back to the 1930's, describe changes in channel networks, and quantify bed level changes and bank erosion rates. We then utilize a calibrated detailed process-based hydrodynamic model to reproduce several of these observations, and subsequently employ an idealized process-based model to further interpret the data and model observations (cf. Hoitink et al., 2020). The observational and modelling results are integrated in a conceptual model relating the response of parallel tidal channels in sediment-rich systems to human interventions through two complex positive feedback mechanisms. We argue that this response is not unique to the southwest GBD and has occurred previously in engineered high-concentration systems, and will also take place in relatively pristine deltas with high sediment loads when subjected to similar human interventions.

2. Tidal amplification and network reorganization: Observations

2.1. The Passur-Sibsa estuary

The long-term mean annual discharge for the combined Ganges-Brahmaputra system is estimated as 3.15 10^4 m^3/s (Jian et al., 2009) transporting about 0.5 billion ton/year of sediment to the sea (Rahman et al., 2018; Paszkowski et al., 2021). Most of this sediment enters the Bay of Bengal in the southeast of the delta through the Meghna outlet. The southwest of the GBD consists of large, parallel tidal channels which evolve into an intricate network of smaller creeks (Fig. 1). This dense channel network is still intact in the Sundarbans, the world's largest and largely pristine mangrove forest, but strongly modified in the polder area north and east of the Sundarbans (Wilson et al., 2017). The Passur-Sibsa estuary (hereafter called the PSE) is a multichannel system within the southwest GBD which flows partly through the Sundarbans and consists partly of a heavily modified delta plain. Approximately 30 km from its mouth the river diverges into the Sibsa River (west branch) and Passur River (east branch). The port of Mongla is situated at the edge of the Sundarbans forest, and is Bangladesh's second-largest port. North of Mongla, the Passur river is connected with the Sibsa river through four connecting channels (see Fig. 1 and Fig. 8). In this study we distinguish three types of tidal river systems: (1) primary rivers (the Passur and the Sibsa tidal rivers, which are typically-one to several km wide), (2) connecting channels (tidal channels linking primary rivers) and (3) blind peripheral channels (tidal creeks draining intertidal areas; historically these channels could be up to 1 km wide).

Due to a very mildly sloping topography (0.016 m/km), tidal waves propagate approximately 200 km inland (Bricheno et al., 2016): 6170 km^2 is less than 2 m above mean sea level and 10500 km^2 is flooded during storm surges (Syvitski et al., 2009). The Sibsa River receives very limited fresh water from upstream and fans out into an intricate channel network of blind peripheral channels. The Passur river receives approximately 10 % of the Ganges river discharge (although the exact amount is not exactly known because of channel bifurcations – see Aziz and Paul, 2015), corresponding to a yearly average of ~1000 m^3/s. Note that for readability we simplify the nomenclature of the various rivers: the Passur river as described in this paper is officially known as the Nobaganga, Rupsha, and Passur rivers (from upstream to downstream). The various river systems in Bangladesh are also known under different names (resulting from different translation of their Sanskrit or Bengali names into English) and therefore our names may differ from other sources. The Passur river, for instance, is also known as Pasur, Pusur or Pussur river.

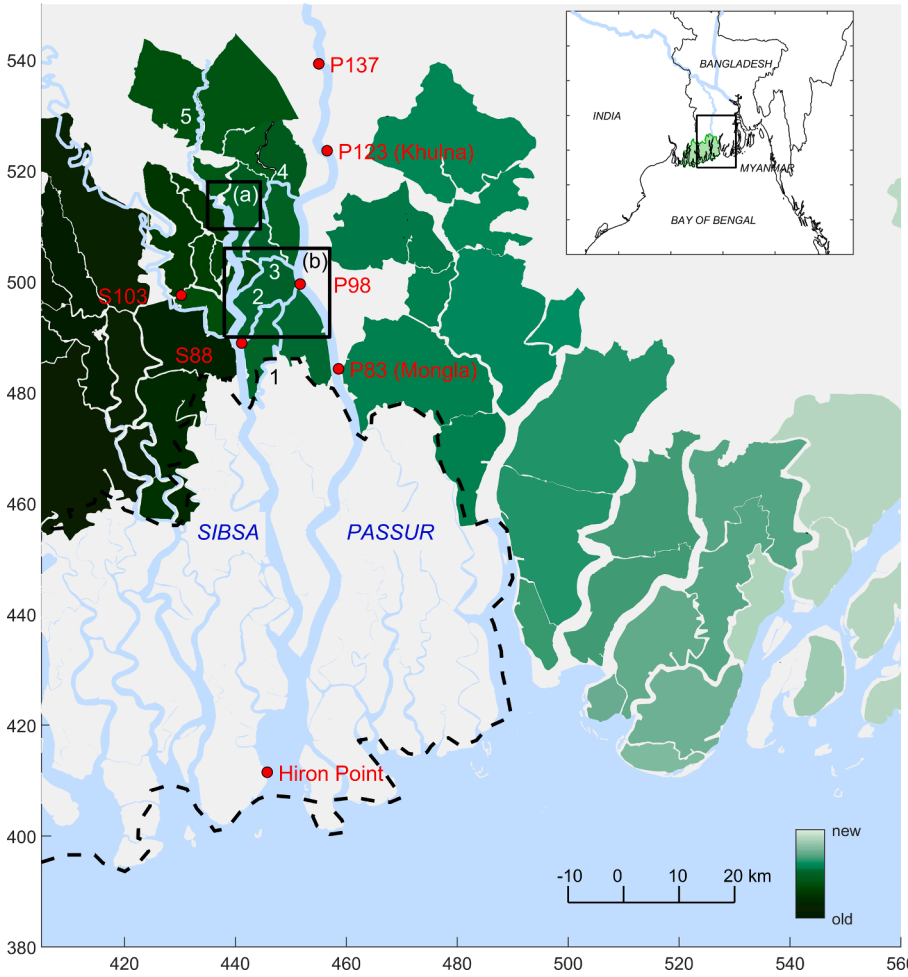

Fig. 1. Map of the Passur-Sibsa basin (in BTM coordinates: Gulshan 303/Bangladesh Transverse Mercator, EPSG 9678, https://epsg.org/crs_9678/Gulshan-303-Bangladesh-Transverse-Mercator.html?sessionkey=vvgl0blset) with water level observation points (red) and names of the river systems discussed in this paper (1: Sutarkhali; 2: Dhaki; 3: Badupgacha; 4: Bhadra; 5: Hari). The green colours depict the chronology of polder development (based on polder number). The contours of the Sundarbans are indicated with dashed lines. The insets (a) and (b) denote the areas detailed in Fig. 8. Inset top right: Larger Ganges-Brahmaputra delta with the Sundarbans in green and the Ganges-Brahmaputra rivers in blue.

The delta plain of the PSE between Khulna and Mongla was still pristine mangrove forest in 1775. Most mangroves were already converted to agricultural land by 1841; the contours of the current Sundarbans forest were already present in 1954 (Nishat et al., 2019). The landscape of this reclaimed land originally consisted of supratidal land and intertidal areas connected with the main rivers through an intricate network of smaller rivers and creeks (so-called peripheral channels). Embankments gradually increased in strength, due to higher human demand for agricultural land, but also due to relative sea level rise. Likely, the embankments progressively moved from the supratidal areas towards the intertidal plains. Embankments were weak, resulting in regular flooding until they were rigorously reorganised in the 1960's to 1970's through construction of coastal embankments. The first polders were developed in the west (dark green in Fig. 1), gradually moving eastward. Unfortunately, exact dates for polder construction are difficult to provide for two reasons. First, existing databases are incomplete and contradictory. Second, the duration of polder improvement differed widely (from several years to several decades), timelines of polder improvement are absent, and the date of polder completion is often stored as the year of polder construction. However, the first improvement is typically to create or raise embankments,which is of primary concern for our analyses. Therefore, the beginning of polder construction is a more meaningful metric. The beginning of polder construction is qualitatively provided by the chronological numbering of polders, indicating the order in which their construction started (1961 for polder 1, 1992 for polder 41/7a). Therefore Fig. 1 provides the chronology of polder construction, but not their exact dates.

An important consequence of polder construction was that the channels draining rainwater from the polders silted up because of a sharp reduction in tidal prism. As a result, despite better protection against moderate storms or fluvio-tidal floods, the polder areas became more vulnerable to both extreme storm conditions and pluvial flooding (water logging) – see Adnan et al. (2019). Silting up of the peripheral channels also negatively impacted navigability, and as we will elaborate in the following sections, also triggered amplification of the tides and large-scale bank erosion.

2.2. Water level observations

The PSE features the area with the densest network of long tidal records in the GBD, operated by the Bangladesh Water Development Board (BWDB) and the Bangladesh Inland Water Transport Authority (BIWTA). All old gauging stations only registered the (visually observed) high and low waters; only several gauging stations switched to hourly (visual) observations or automatic registrations in more recent years. This data is sufficiently accurate to investigate long-term changes in tidal dynamics, and provides crucial information on historic changes (Fig. 2).

The tidal range has increased slowly between 1940 and 1960, and accelerated after ~1960 (Fig. 2; middle panels in Fig. 3). This increase in tidal range leads to higher high waters (Fig. 2; top panels in Fig. 3): for stations P123 (Khulna) and P98 (stations with the longest available water level recordings) the annual high water increased from approximately 2 m above PWD in 1940 to almost 4 m in 2015. The tidal mean water elevation has increased by not more than 0.5 m over the duration of the observations (lower panels in Fig. 3), resulting from relative sea

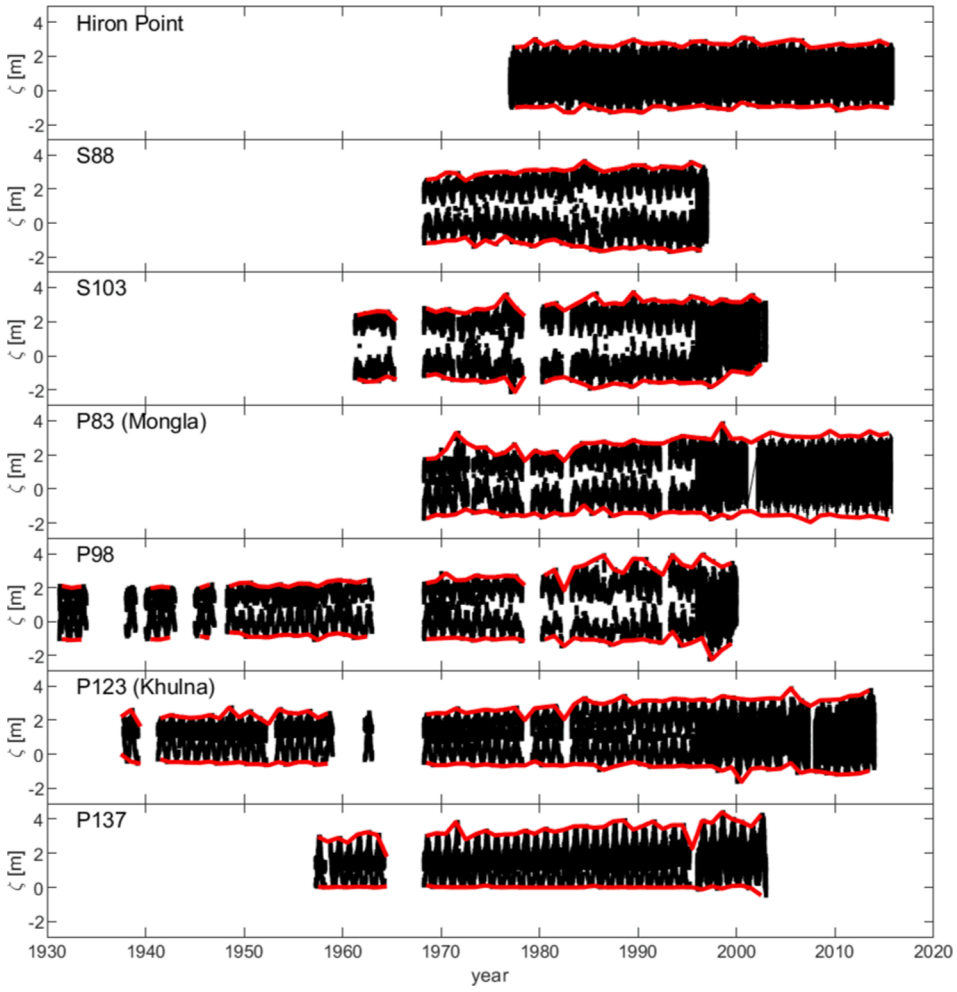

Fig. 2. Observed water levels (ζ) in the Sibsa and Passur rivers. The original gauging station names have been converted to a physically more meaningful name including the name of the river (P for Passur and S for Sibsa) and their distance from Hiron Point (the gauging station in the mouth). The formal name of station S88 is SW29, S103 is SW256, P98 is SW243, and P137 is SW219. All water levels are relative to Public Works Datum (PWD: http://www.sob.gov.bd/site/page/5c483297-6269-4111-a6c3-4a15cce85844/). The red line is the envelope of the annual lowest and highest water levels. Data provided by the Bangladesh Water Development Board (BWDB) and the Bangladesh Inland Water Transport Authority (BIWTA).

level rise (RMSL; a combination of eustatic sea level rise and subsidence). Only S103 experienced a rapid increase in RMSL in the end of the 1990's, resulting from infilling of the river channel wherein the gauging station was located. In contrast, the tidal range increased much more: over 2 m at P98 and P123 (middle panels of Fig. 3). The tidal range at the mouth of the PSE (Hiron Point) remained constant, implying that all tidal changes within the PSE are caused by internal dynamics and not by offshore forcing. These internal dynamics are further examined by defining a tidal amplification as the ratio of the tidal range (per station) divided by the average tidal range measured at Hiron Point (shown in Fig. 4 for the period between 1969 and 2020; the period for most data was available). Tidal amplification started in the Sibsa estuary (already since the 1960's) but stopped around 1985. In contrast, tidal amplification in the Passur accelerated after 1982. We hypothesize, as will be explored in more detail in sections hereafter, that this asynchronous tidal amplification is caused by the temporal order at which these polders were constructed or on the different relative reduction in size.

Fig. 3 and Fig. 4 contain four crucial observations for understanding human impacts on the dynamics of the PSE, being that (1) high water levels increase predominantly because of tidal amplification rather than because of relative sea level rise, (2) tidal amplification in the Passur is progressing linearly and shows no signs of slowing down, (3) tides also amplified before polder construction, albeit at a lower rate, and (4) tidal amplification started in the Sibsa (and continued until the mid-1980's) and was followed by the Passur (starting in the early eighties).

2.3. Shoaling and bank erosion in the primary channels

The Passur river seaward of the connecting channels (between BTM Y = 450–500 km) is silting up (Fig. 5b). This shoaling is evidenced by detailed surveys executed in 2011 and 2019, with deposition rates exceeding 0.3 m/y (Fig. 5b). Deposition was already reported to be structural since the 1990's, with peak annual deposition rates varying longitudinally between 0.2 and 0.9 m/year (Rahman, 2017; Rahman and Ali, 2018). However, structural deposition started well before the 1990's, as evidenced by cross-section observations near Mongla (inset of Fig. 5): the maximum depth decreased 71 % (from 21 m to 6 m) between 1973 and 2003 (data from the Bangladesh Institute of Water Modelling (IWM), 2003). Other areas in both the Passur and Sibsa rivers display lateral variability in erosion and sedimentation typical for tidal systems, without an apparent trend in erosion or accretion within the short time span of observations (8 years).

Longer timeseries of channel dynamics are provided by extracting riverbank positions from satellite images. For this purpose, nine satellite images covering the period 1988–2019 were manually digitized (Fig. 5c). Herein riverbank positions are clearly identified as local embankments (along dynamic coastlines, where new land is either rapidly reclaimed or retrograding coastlines are protected), permanent embankments (stable coastlines) or the vegetation margin (in the Sundarban forest). The riverbank locations were converted into channel widths along the channel thalweg, which were subsequently used to compute the relative change in channel width per year, using the first observation in 1988 as a reference year (Fig. 6). This data shows that the Sibsa rivers widened up to between 200 and 400 m in the section between the

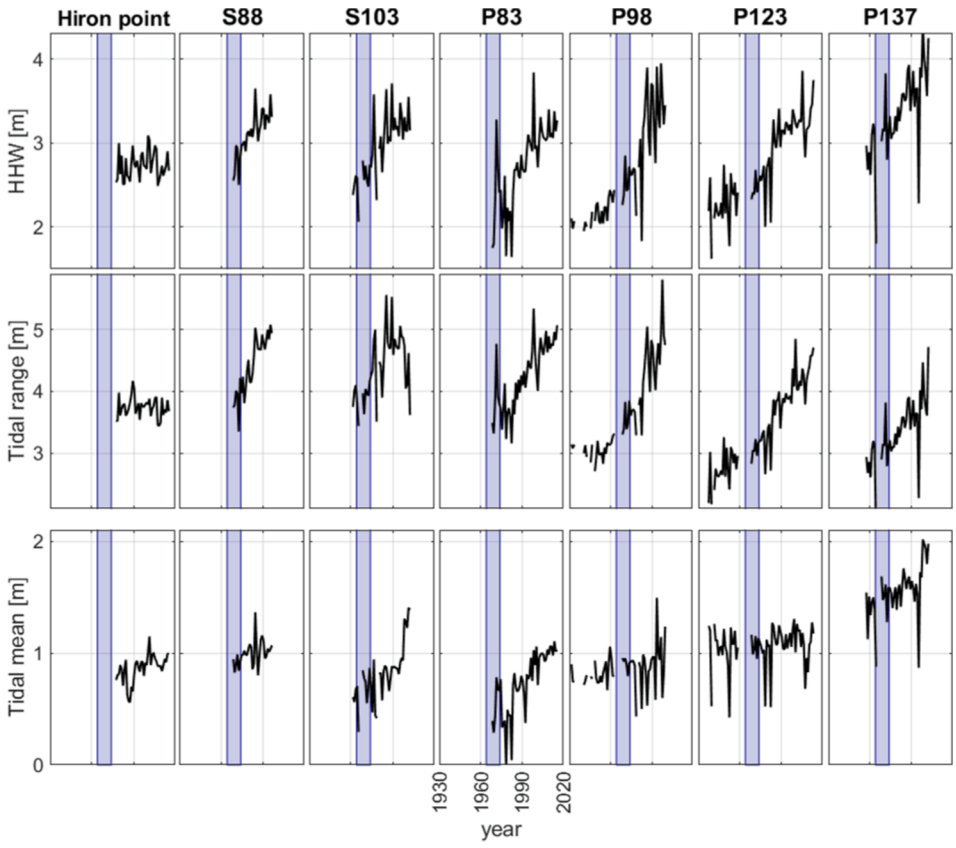

Fig. 3. Higher high water (HHW), tidal range, and mean water level at the 7 gauging stations of the Passur-Sibsa river, from 1930 to 2020. The purple bars denote the period of large-scale improvement of coastal embankments, often coinciding with gaps in water level data. Data provided by the BWDB and BIWTA.

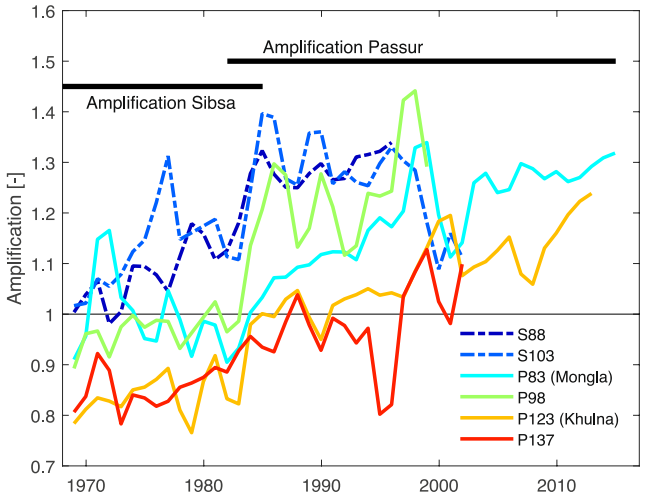

Fig. 4. Amplification (defined as the tidal range for all stations (except Hiron Point) shown in Fig. 3) divided by the long-term average tidal range at the mouth, i.e. Hiron Point). Data provided by the BWDB and BIWTA. The rapid reduction in tidal amplitude at station S103 (shortly before it was discontinued) is caused by rapid infilling and abandonment of the channel in which the gauging station was located.

estuary mouth and the most landward connecting river (the first 100 km; Fig. 6a). Averaged over the entire section seaward of the connecting channels, the Sibsa has widened 15 % over a period of 30 years (Fig. 7a); compared to 1937 this widening was substantially larger (see the supplementary information). Landward of the confluence zone (x >100 km), the channel width decreased rapidly: 20 % between 1988 and 2001 but stabilising afterwards (Fig. 7a).

In the Passur, the channel width landward of the connecting channels and partially in the area where connecting channels are located (between km 105 and 130; Fig. 6b) increased, averaging 15 % (Fig. 7a). Just north of Mongla (km 85–105), the channel became narrower while it widened again in the most downstream 80 km (5 %; see Fig. 7a). Apparently, the channel section in-between gauging stations Mongla and P98 (where the Passur joins the Sutarkhali-Dhaki connecting channels) becomes narrower and shallower. The erosion of the Sibsa river may be partly attributed to an increase of the tidal prism through flow capture of the Sibsa from the Passur (Bain et al., 2019). However, this channel capture is probably insufficiently extensive to explain the large bank erosion rates. Even more, the discharge through the Passur has decreased as a result of channel capture whereas the Passur riverbanks erode as well (albeit at a lower rate). We hypothesize that the decrease in tidal discharge through loss of intertidal area is compensated by an increase in tidal amplification. The surface area of the Sibsa river between its head and its confluence with the Passur is 163 km^2; an increase in tidal range of 1 m (a conservative estimate since the tidal range in both S88 and S103 is more – see Fig. 3) increases the tidal volume with 163 10^6 m^3. The Sundarbans area draining into the Sibsa along this same stretch is 772 km^2, resulting in a 772 10^6 m^3 larger tidal volume. However, the bed levels of the Sundarbans keep up with the increase in peak water levels (Auerbach et al., 2015; Bomer et al., 2020) while the tidal range becomes reduces towards the more distal intertidal areas of the Sundarbans. Therefore, the increase in tidal prism is less than what may have been expected for open channels. Since the Sundarbans creeks largely follow the increasing highwater levels of the Sibsa river, we assume that the increase in tidal prism is 20 % of 772 10^6 m^3, corresponding to 154 10^6 m^3. The resulting total increase in tidal prism is therefore estimated to be 314 10^6 m^3, exceeding the loss in volume by polder construction in the Sibsa (estimated by Bain et al. (2019) to be

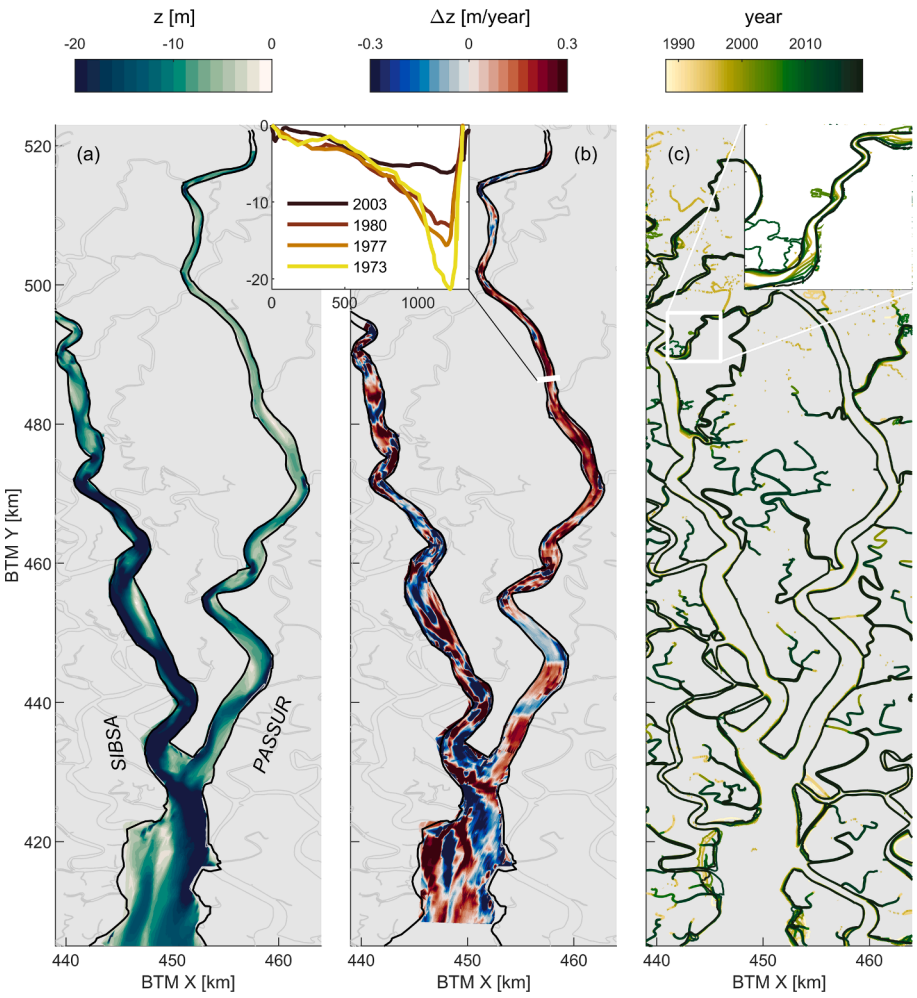

Fig. 5. Bed level (in meter below PWD) of the PSE in 2019 (a) and the annual increase in bed level between 2011 and 2019 (b). The inset between (a) and (b) visualizes cross-sectional bed levels measured at Mongla Port (location indicated with the arrow in panel (b), with channel width and depth in meters). Panel (c) provides coastlines digitized from Landsat satellite images USGS Earth Explorer over the period 1988 (yellow) – 2019 (dark green), with the inset exemplifying details of coastline changes within a connecting river. Bed level data in (a) and (b) is from IWM; bed level data at Mongla is digitized from IWM (2003). Note that for readability the aspect ratio of the map is not 1:1.

153–246 10^6 m^3). This phenomenon also explains the progressive erosion rates in the seaward direction in Fig. 6: in the upper estuaries the effect of loss of intertidal area exceeds or compensates tidal amplification. In the lower reaches tidal amplification dominates, because tides in the Sundarbans area amplified whereas no land was reclaimed.

2.4. Channel network reorganization

The construction of polders in the 1960's to 1980's reduced the tidal prism in the PSE with 209–302 10^6 m^3 (Bain et al., 2019). An important consequence of minimising flooding through construction of the embankments was that the tidal discharge conveyed by the blind peripheral channels sharply decreased. With an abundant supply of fine-grained sediments, the blind peripheral channels silted up (exemplified by Fig. 8a). Over 1000 km of peripheral channels filled up with sediments in the embanked part of the southwest GBD, and to date, 16 km of channels are still converted to land every year (Wilson et al., 2017). The present-day rate of channel closure is therefore comparable to average infilling rates since the 1970's (around 20 km/year).

In contrast to these blind peripheral channels, the channels connecting the Sibsa and Passur rivers are widening (Fig. 8b). Parts of the Dhaki and Badupgacha rivers are not drawn on the 1937 map, suggesting they did not exist or were minor creeks. The change in channel width can be explored in more detail using the satellite-based images showing riverbank positions for the connecting channels as well. Using this method, the average channel width increase in the connecting channels is estimated to be from ~10 % in the Bhadra River (the most Northern connecting river) to 60 % in the Dhaki River (Fig. 7b). The Dhaki river widened from close to 0 in 1937 to ~200 m in 1988 to almost 400 m wide in 2019, becoming a major tidal channel.

Summarizing, the tides in the PSE amplify, the Sibsa river and connecting channels widen, and up to the confluence with the connecting channels the Passur river degenerates. The speed of all these changes is almost constant, and there is no evidence of declining rates of channel infill, bank erosion, or tidal amplification.

3. Tidal amplification and network reorganization: Modelling

3.1. Scenario-based model analysis

A depth-averaged, process-based, hydrodynamic model of the Passur-Sibsa estuary is developed, representing present-day conditions (see details in the supplementary material). The model is setup in Delft3D using a curvilinear grid, solving the unsteady shallow water equations under the hydrostatic pressure assumption (Lesser et al., 2004). The seaward boundary of the model is Hiron Point (see Fig. 1), where continuous water level observations are available to prescribe as model boundary conditions. The up-estuary boundary is defined as the zone where tidal discharge becomes sufficiently small to have a minor impact on the tidal dynamics within the PSE. The up-estuary boundary conditions are obtained from existing flood prediction models, consisting of tidal water level variations but also river discharge time-series. The only distributary receiving a significant freshwater input is the Passur River (connected to the Ganges River through the Gorai River), varying between 0 (dry season) to 3000 m^3/s (wet season).

The bathymetry of the main rivers is based on topographic transect

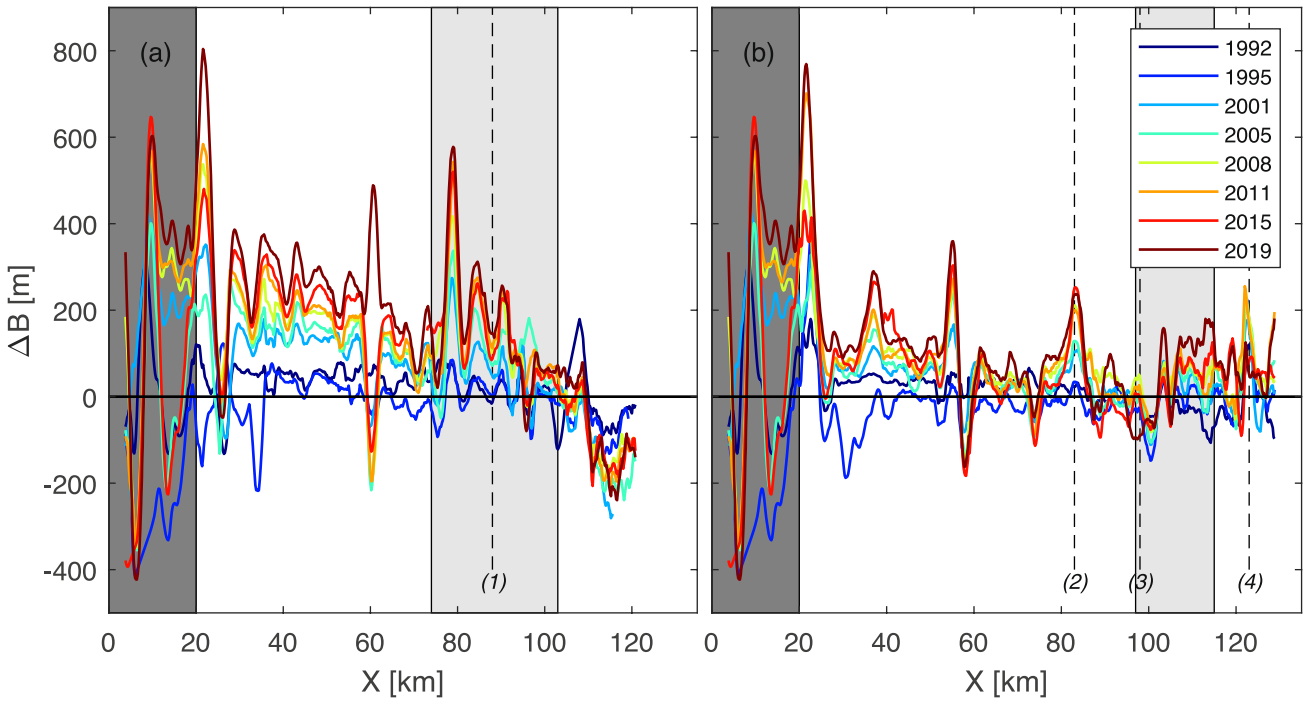

Fig. 6. Change in channel width ΔB (in m, relative to the channel width in 1988) in the Sibsa (a) and Passur (b) rivers, derived from the satellite images in Fig. 5c. Light grey shading indicates the channel section drained by connecting channels, dark grey shading the joint Passur-Sibsa channel. The numbers refer to the location of gauging stations, where 1 = S88, 2 = P83 (Mongla), 3 = P98, and 4 = P123 (Khulna).

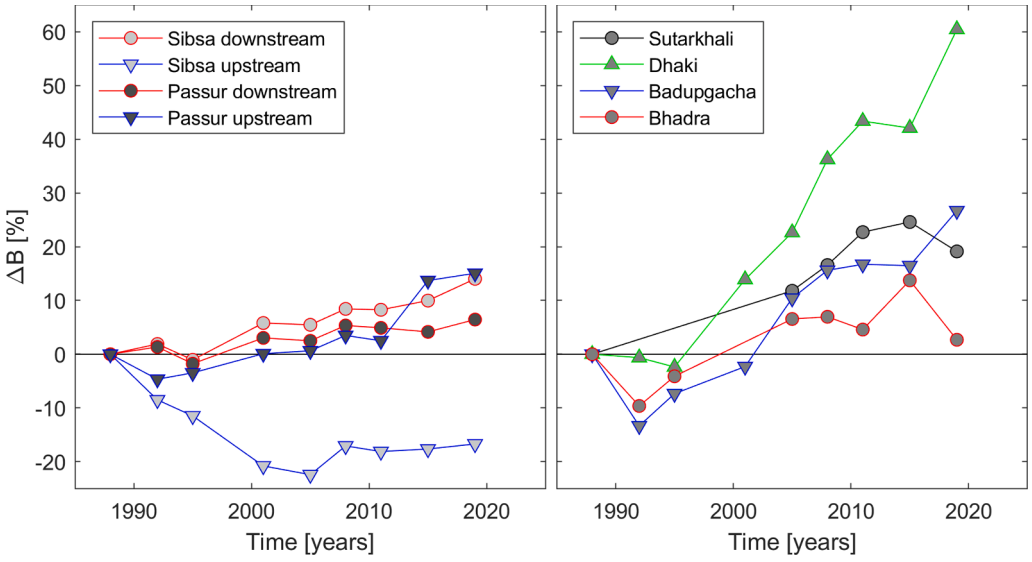

Fig. 7. Change in average channel width ΔB (with an increase defined positive) relative to the channel width in 1988 of the main distributary channels (a; upstream and downstream of the area with connecting channels) and of the four connecting channels themselves (b). ΔB is defined as the along-channel average of the longitudinal change in width (per year) and derived from the satellite images in Fig. 5c.

data. The Passur river is shallower than the Sibsa River (Fig. 5a). The channel deepens again in the upper Passur, probably related to the channel network switching elaborated above. No detailed bed level data is available for the intertidal part of the Sundarbans but it is approximately equal to Mean High Water (Auerbach et al., 2015, Hale et al., 2019a), and therefore the bed level of the vegetated parts of the Sundarbans is set to 2 m above MSL. Mangroves lead to a reduction in flow velocities, implemented using the formulations developed by Baptist et al. (2007). The model is calibrated against continuous water level observations (Fig. 9) and through-tide discharge measurements (see supplementary materials) by varying the hydraulic bed roughness, resulting in an optimized Manning's n of 0.015 s/m$^{1/3}$.

The model is subsequently used to better understand historic developments on the delta plain. Unfortunately, there is insufficient data to fully reconstruct pre-polder conditions: bed level surveys of the supra- and intertidal delta plain and tidal channels were not executed (or preserved) with sufficient accuracy and spatial detail. The current bed levels of the delta plain cannot be used for historic hindcasts because of the large degree of anthropogenic reworking and subsidence. We therefore define four quasi-historic scenarios which are largely based on present-day conditions but do provide insight into historic changes:

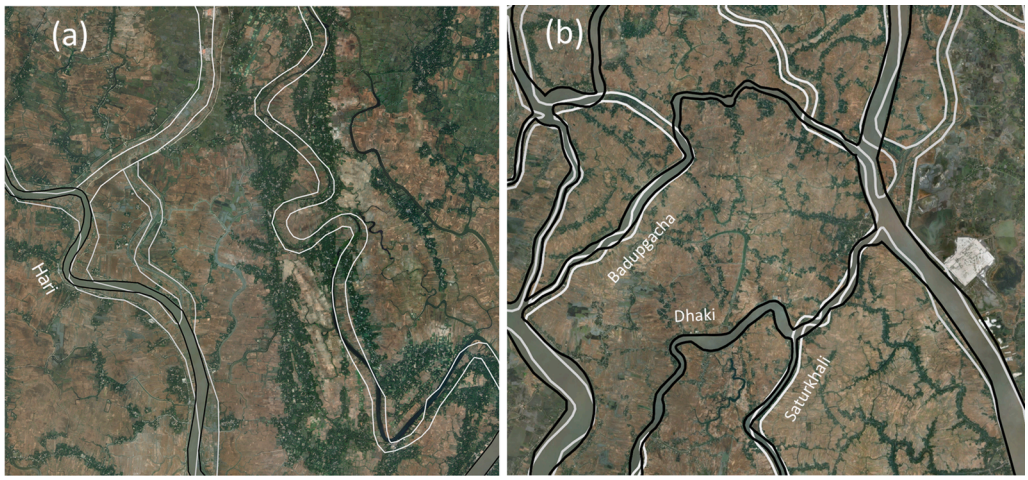

Fig. 8. Satellite image (2020) in an area with primarily infilling channels (a) and newly developing connecting channels (b): see Fig. 1 for locations. The black lines provide the 2020 riverbanks (digitized in QGIS from the 2020 satellite image) whereas white represent riverbanks in 1937. The 1937 riverbanks are digitized in QGIS from the Bengal, No 79F, Khulna (IOR_Y_79F_1937) map by the Survey of India, made available by the http://britishlibrary.georeferencer.com and accessed via www.davidrumsey.com. See the supplementary Information for more details on the 1937 map.

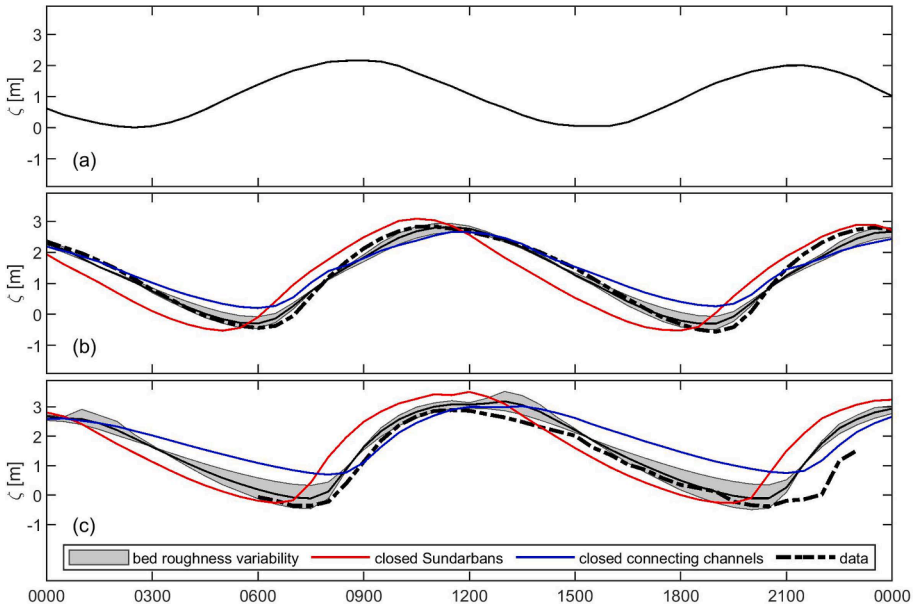

Fig. 9. Observed (black dashed line) and modelled water levels in Hiron Point (a), Mongla (b) and Khulna (c), on 27 August 2011. Water levels are computed using three Manning's roughness values: 0.15 s/m$^{1/3}$ (black line) and 0.12–0.2 s/m$^{1/3}$ (grey shading) and for two alternative secondary channel configurations: without Sundarbans (red line) and without channels connecting the Sibsa and Passur (blue line).

1. The impact of the loss of intertidal areas and infilling of creeks on tidal dynamics is approximated with an analysis of the present-day Sundarbans. We assume that closure of the intertidal area of the Sundarbans represents the initial phase of land reclamation, and that an additional closure of its channels represents the final phase of reclamation (in which peripheral channels have silted up).
2. The role of the connecting channels on tidal dynamics is evaluated by running the model with and without flow through the connecting channels, representing present-day conditions and the period before large-scale land reclamations, respectively.
3. The river discharge from the Ganges River to the Passur Estuary (via the Gorai River) may be gradually decreasing: the wet season discharge of the Gorai River was about 50 % larger in 1980 compared to the present situation (Anwar et al., 2020). However, at the same time the distribution of the Gorai discharge to the Passur probably increased. At present, 85 % of the Gorai River discharges into the Passur River (Aziz and Paul, 2015) while this was probably around 50 % before polder construction (NEDECO, 1967). Still, in order to differentiate between the potential impact of discharge reduction and land reclamations, the model is additionally run with a 50 % higher river discharge.
4. The available bathymetric data reveal that the Passur is rapidly shoaling and was much deeper before the large-scale land reclamations. In order to isolate the impact of infilling of the Passur River, we define a scenario with a deeper Passur channel. Herein, the bed of the Passur River is lowered with 50 % of its present depth near Mongla (the area where sedimentation rates appear to be maximal), gradually fanning out to 0 % at the connection with the Sibsa River and the Surkhali River.

The alternative scenarios are evaluated with the spatial distribution of the M2 amplitude (the main tidal constituent), computed from the model results with the *T*-tide toolbox (Pawlowicz et al., 2002).

Closure of the Sundarbans intertidal areas (representing the instantaneous impact of land reclamations) leads to tidal amplification in the Passur river (Fig. 10). Intertidal flats provide storage for the incoming tidal wave and an energy loss term, both dissipating the tidal wave. Reclaiming the intertidal area therefore leads to tidal amplification

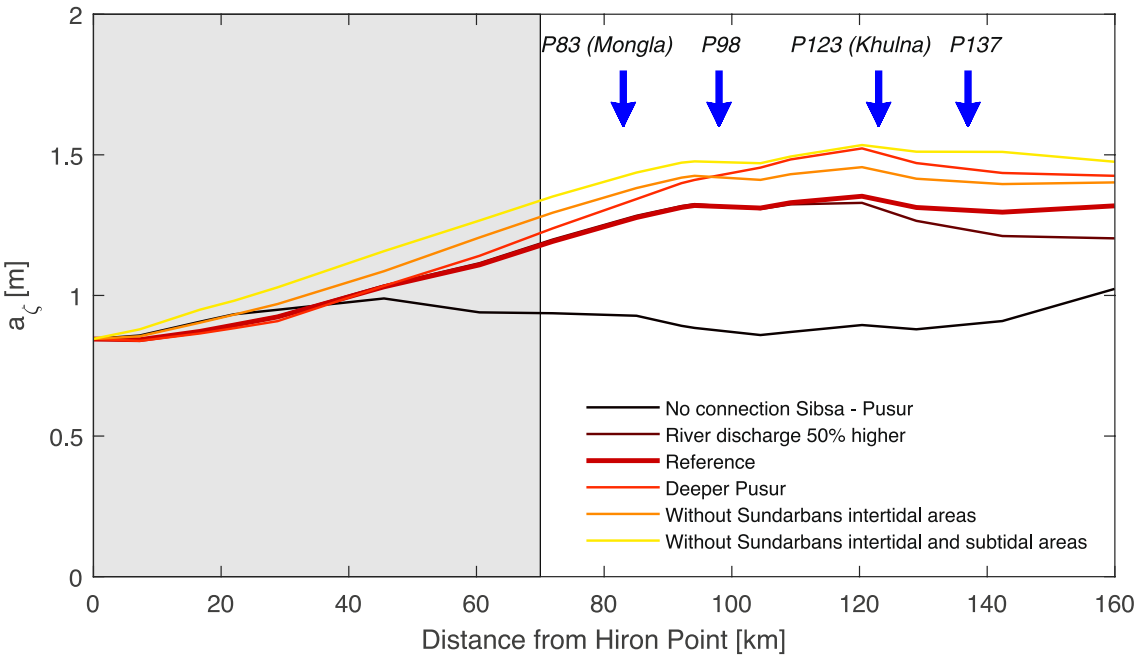

Fig. 10. Modelled amplitude of the M2 tidal constituent in the Passur basin for the reference simulation and five alternatives (see legend and text). The dark shades indicate the location of the Sundarbans forest; the light gray areas (with dashed lines) the area with connecting peripheral channels; the arrows with text the locations of the water level stations.

(Song et al., 2013; Winterwerp and Wang, 2013). Using the Sundarbans as an approximation of the historic delta plain provides a lower bound for the impact of loss of intertidal area because the further upstream the intertidal area is located, the stronger its loss contributes to tidal amplification (Li et al., 2016). But most importantly, the additional infilling of the tidal channels leads to an amplification of the tides similar to the contribution of the intertidal area alone. This reveals that the infilling of tidal channels has a large impact on tidal dynamics. We expect the effect of tidal channel closure in the Sundarbans (as in the model) is comparable to the effect of infilling of the blind peripheral channels on the reclaimed delta plain (as described by Wilson et al., 2017; see also Fig. 8a). This means that the infill of these blind rivers is probably an important mechanism explaining the observed continuous tidal amplification after the initial reclamation (Fig. 3).

The model scenario with the largest impact on tidal amplification is the closure of the connecting channels. Both Fig. 9 and Fig. 10 reveal that flow through the connecting channels leads to tidal amplification in the Passur River, up to 45 %. When the connecting channels widen (Fig. 7), more tidal discharge is conveyed from the Sibsa to the Passur, and tides in the Passur amplify (Fig. 3): tides in the Sibsa River capture the inland part of the Passur.

A tidal wave is damped by the upstream river discharge (Sassi and Hoitink, 2013; Guo et al., 2015), resulting in lower tidal amplitudes for the scenario with a higher river discharge. However, the impact of the river discharge is confined to the river section upstream of km 120, only influencing gauging station P137. Therefore, the reduction in river discharge presumably influenced the most upper reaches of the Passur river, and not the Passur near Khulna or Mongla. Finally, the scenario with a lowered riverbed (compared to its present level) leads to higher tides in the upper Passur river. This further illustrates the progressive decline of the Passur River, because during the period the Passur became shallower the tides actually amplified. Channel capture provides the most realistic explanation for this disparity.

The scenarios suggest that the tides initially amplified by reclamation of intertidal areas, but in a later stage amplified because the blind peripheral channels filled in due to flow diversion through the connecting channels. A potential reduction of the freshwater river discharge may have had an additional effect, but only in the upper river. The infilling of the Passur river near Mongla provides a component leading to damping of the tidal wave propagating through the Passur, thereby strengthening flow capture by the Sibsa (amplifying the tides). The relationships elaborated above explain how tidal dynamics are related to the river channel network, dimensions, and river discharge but they do not explain why the Sibsa captures the storage space in the upper Passur (instead of vice versa). Which channel becomes dominant (and captures tidal storage from the other) is determined by relative water level gradients, which are the result of asynchronous changes in the propagation speed and amplitude of the tidal wave.

3.2. Tidal propagation speed

The tidal wave propagation celerity c is approximated by $\sqrt{gh}$, with h the water depth and g the gravitational acceleration, showing that tides propagate faster in deeper channels than in shallow channels. The present-day Sibsa River is deeper than the present-day Passur River and therefore, the tidal wave propagates much faster through the Sibsa River (11.2 m/s) than through the Passur River (8.1 m/s) (Bain et al., 2019). The resulting time-varying water level gradient drives a flood flow from the Sibsa to the Passur in the dry season (Shaha and Cho, 2016). Using the (average) channel depth, the travel time from Hiron point to P98 (see Fig. 1) through the Passur branch, the Sibsa- Sutarkhali branch and Sibsa-Dhaki branch is estimated at 115, 108, and 101 min (respectively). The travel time through the Passur River is therefore longer than through the connecting channels. These travel times explain the present-day tidal channel capture of the upper Passur River. However, the Passur River is filling up rapidly (Fig. 5) and therefore the channel was deeper when channel capture started. Therefore, channel depth and the associated tidal wave propagation speed do not explain the onset of flow capture. Likely, this initial change was triggered by bathymetric constraints imposed by land reclamations and polder construction.

The characteristics of a tidal wave propagating through an estuary flanked by intertidal areas is influenced by the intertidal areas by providing storage (Friedrichs and Aubrey, 1994) and an additional source of friction (Stark et al., 2017). Loss of intertidal areas therefore

not only influences the amplitude and asymmetry of the tidal wave, but also its propagation speed. When closing the Sundarbans, for instance, the tidal wave arrives 30–60 min earlier at Mongla and Rupsha (Fig. 9b, c). To evaluate the impact of channel depth and the intertidal storage on the tidal propagation speed, we develop an idealized Delft3D model of a funnel shaped estuary based on the dimensions of the Sibsa River, from the estuary mouth to the point where the Sibsa rapidly decreases in width, and bifurcates into a number of smaller branches. The channel width w is obtained by fitting $w = w_0 \exp(-l/L_c)$ to the Sibsa channel, yielding a convergence length L_c of 50 km for a channel width w_c at the estuary mouth w_0 of 7 km (Fig. 11a). The bed level z of the present-day Sibsa River decreases from approximately 20 m below MSL at the mouth to 10 m at the landward end (90 km from Hiron point, where the main channel trifurcates into smaller blind peripheral channels), which is prescribed as a linearly sloping bed level profile (Fig. 11b). We expect that the channel was shallower before polder construction because of the tidal discharge captured from the Passur system eroded riverbanks (Fig. 6a, Fig. 7a), and therefore probably also the river bed. We assume that the riverbed at the landward end is 30 % shallower (7 m), and that the mouth region is only marginally shallower (5 %; 19 m). The shallow channel scenario is also evaluated with an intertidal area W_i (width of intertidal area) equal to w_c, (width of the channel) which is symmetrically split over the opposite sides of the channel. The modelled intertidal area represents both the intertidal area and the intricate pattern of tidal creeks that were historically present, as exemplified by the present-day Sundarbans mangrove forest, and therefore it has been assigned a bed level Z_i increasing from −0.8 m to 0.8 m (Fig. 11c). Since $W_i = W_0$ and the average Z_i equals MSL, the tidal storage of the tidal flats is approximately half the tidal storage of the channel.

We evaluate the propagation speed of an M2 tidal wave with an amplitude of 1.5 m. We impose a weakly reflective boundary condition (Riemann invariant) at the landward boundary, to prevent numerical tidal amplification.

The three scenarios defined in Fig. 11 represent a chronological sequence of land reclamations in the Sibsa River. The original depth with intertidal areas corresponds to pristine conditions, followed by a loss of intertidal areas resulting from land reclamations (i.e., polder construction), which in turn is followed by a deepening of the tidal channel, because of the larger tidal prism. The model runs (Fig. 11d) demonstrate that the propagation speed is much more sensitive to the presence of intertidal areas than to an increase in the depth of the main channel. The reason for this is that in areas with substantial intertidal areas the tidal celerity is not $c = \sqrt{gh}$ (as in single channels) but $c = \sqrt{gA_t/w_t}$ (with A_t the cross-sectional area and w_t is the total width). This has important implications for the Passur-Sibsa basin. Polders were first constructed along the west bank of the Sibsa, followed by the delta plain in-between the Sibsa and the Passur, followed by the east bank of the Passur (Fig. 1). Additionally, a larger amount of intertidal area was reclaimed in the Sibsa compared to the Passur. As a result, the tides started amplifying more and propagating faster in the Sibsa River before these developments occurred in the Passur River (see also the asynchronous tidal amplification in Fig. 4). This allowed the Sibsa basin to capture tidal storage space from the upper Passur River, resulting in infilling of the lower Passur River and deepening and widening of the Sibsa River and its connecting channels. The moment the Passur basin was also reclaimed, the system had already become subordinate to the Sibsa River because of its smaller depth.

4. Discussion

4.1. Positive feedback mechanisms amplifying tides, channel shoaling and bank erosion

Based on our observations and model results, we identify-two positive feedback mechanisms in the tidal response to land reclamations (schematized in Fig. 12). Both mechanisms are dependent on the abundant availability of fine-grained sediments, leading to infilling of the blind peripheral channels and the lower section of one of the main distributaries, the Passur.

The first positive feedback mechanism is tidal amplification in response to progressive infilling of blind peripheral channels (Fig. 12a-

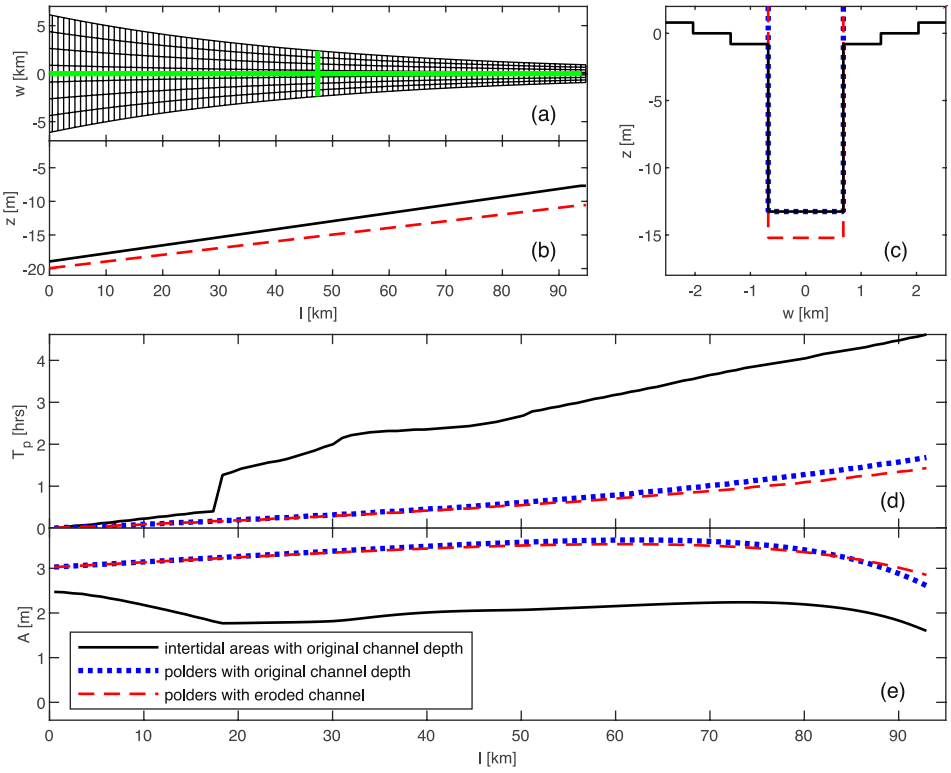

Fig. 11. Travel time T_p (d) and amplitude A (e) of a tidal M2 wave in a funnel-shaped estuary with length L and width w. The model domain (a) is based on the dimensions and convergence of the Sibsa Estuary (see text for details). The green lines in panel (a) provide the location of the longitudinal channel depth (b, in meter below MSL) and the channel cross-section (c). The original depth is a channel decreasing from 19 to 7 m; the eroded channel depth decreases from 20 m at the mouth to 10 m (b). An intertidal area is defined as a platform with a height equal to Mean Sea Level at the mouth (0 m – see (c)) - the intertidal area is absent for polder scenarios.

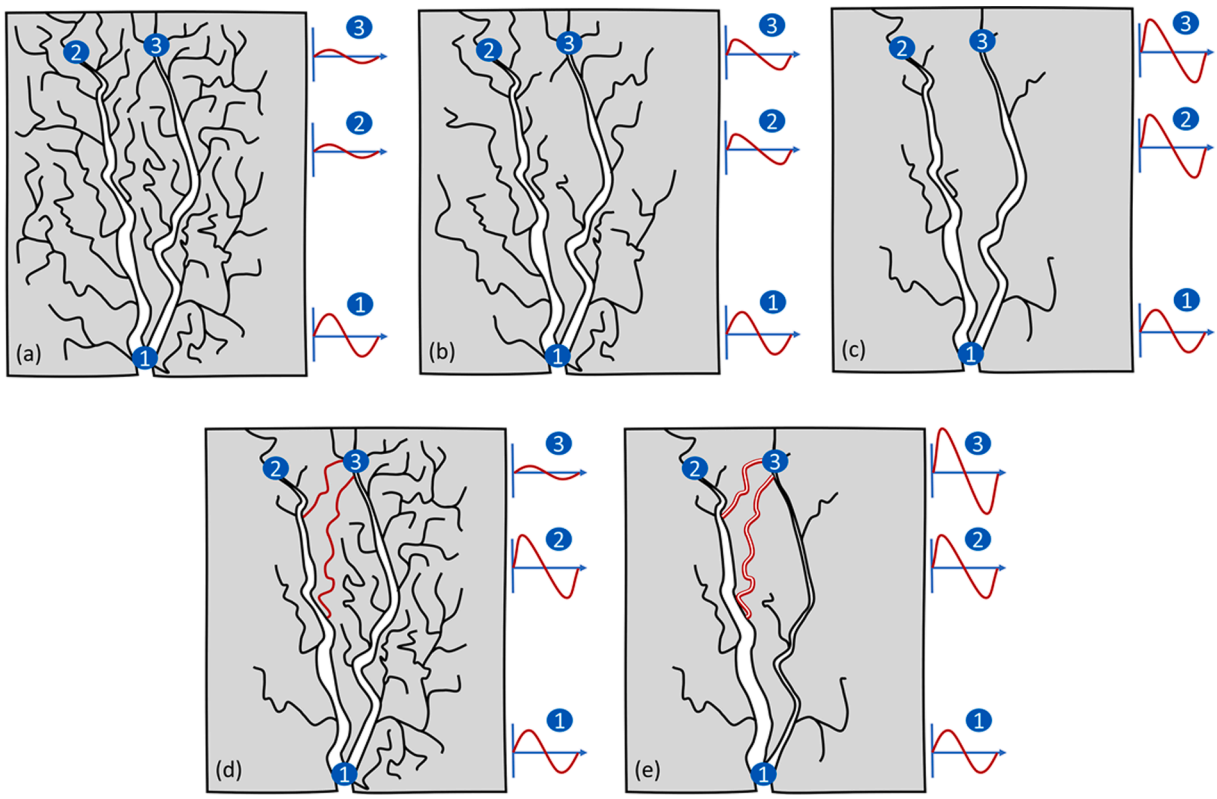

Fig. 12. Positive feedback mechanisms leading to tidal deformation and channel network reorganization. Tides dampen in the up-estuary direction of an initially pristine tidal network (a). Loss of the intertidal area leads to tidal amplification (b), which is progressively amplified by infilling of blind peripheral channels (c). When the intertidal area of two branches are not simultaneously reclaimed, the tides only amplify and deform in the first reclaimed branch (d). Tides penetrate into the pristine channel through smaller connecting channels, leading to amplification of the tides there (e). The connecting channels and the first branch expand while the second branch degenerates.

c). After construction of polders (Fig. 12b), the tides in the main channels amplify (Pethick and Orford, 2013) and deform because of reduced dissipation of the tidal wave (Sundarbans intertidal scenario in Fig. 9 and Fig. 10). Without morphological adaptation, such a response is instantaneous. But because of the high sediment availability, the blind peripheral channels fill in (Fig. 8a), for two reasons. First, the loss of tidal prism from the former intertidal areas leads to a reduction of flow velocity amplitudes in the blind peripheral channels (as described by Wilson et al., 2017). Secondly, the tidal wave in the main tidal channels becomes increasingly flood-dominant because of the loss of intertidal areas (cf. Friedrichs and Aubrey, 1988); sediment is therefore more efficiently transported landward, towards the blind peripheral channels. Infilling starts at the head of these tidal rivers (where the relative reduction in flow velocity is highest), further reducing the tidal prism and flow velocity amplitudes, and hence promoting down-channel infilling. Throughout the GBD, 16 km of peripheral river length silts up per year (Wilson et al., 2017). Crucial to feedback mechanisms 1 is that the loss in tidal prism resulting from infilling of peripheral rivers promotes tidal amplification in the main distributaries which is revealed by the difference between the Sundarbans full and Sundarbans intertidal scenario in Fig. 10. This mechanism is slow, as demonstrated by the almost linear increase in tidal range for 50 years after polder construction (Fig. 3).

The second feedback mechanism explains tidal amplification and riverbank erosion resulting from channel reorganization (Fig. 12a, d, e). Polder construction along one branch (the Sibsa) accelerated the tidal propagation speed in the Sibsa river (Fig. 12d). Water level observations suggest that this channel capture started in the early 1980's (Fig. 4). Both systems are connected through small connecting channels. As a result of the difference in tidal propagation speed between the two channels, water level gradients develop between both distributaries driving a flood flow from the Sibsa to the Passur during flood and in reverse direction during ebb. The connecting channels erode (Fig. 7, Fig. 8b), further promoting tidal amplification in the Passur River, as visible in the connecting channels scenario in Fig. 10, and schematized in Fig. 12e. The lower reaches of the Passur silt up (Fig. 5b) as a consequence of a loss of tidal prism while the river landward of the connecting channels widen (Fig. 6b). The Sibsa river seaward of the connecting channels erodes because of an increase in tidal prism; the Sibsa landward of the connecting channels degenerates (Fig. 6a). Tidal flow through the Passur therefore progressively declines while tidal flow through the Sibsa progressively increases. Without maintenance dredging, the Passur may become a degenerated branch, with a tidal divide in-between the port of Mongla and the connecting channels (corresponding to the area with high siltation rates in Fig. 5b).

The impact of polder construction on bank erosion, pluvial flooding and reduced navigability through tidal amplification is conceptualized in Fig. 13. Pluvial flooding of polders is primarily the result of poor drainage of rainwater because of infilling of the blind peripheral channels, which is aggravated by tidal amplification. Bank erosion is a natural process in a tidal network system, where outer banks erode and inner banks accrete. However, polder construction and bank erosion led to a more structural type of erosion. Part of this structural erosion directly results from tidal amplification, leading to higher flow velocities, yet the most important contributor to bank erosion in the PSE is channel network reorganization. Channel network reorganization leads to bank erosion along the connecting channel and the dominant distributary (the Sibsa), and to shoaling of the Passur river (especially near and North of the Port of Mongla).

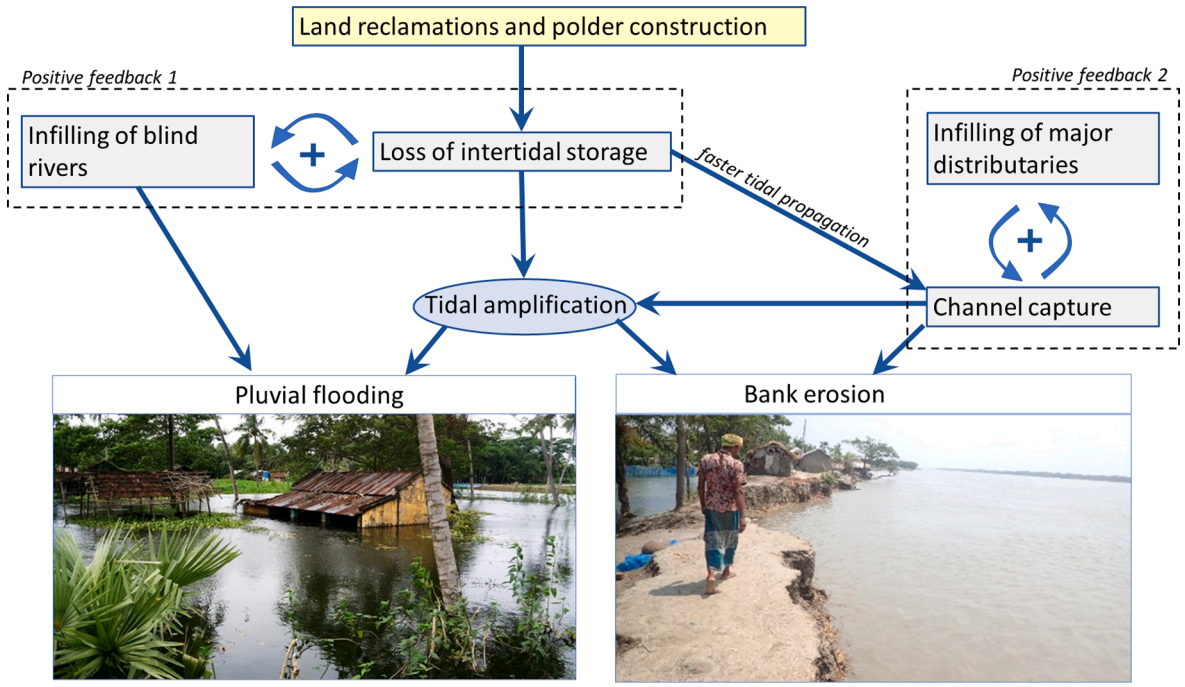

Fig. 13. Conceptual diagram relating land reclamations and polder construction to tidal amplification, bank erosion, and pluvial flooding through two positive feedback mechanisms. See text for details. Left photo courtesy or IWM, right photo taken by the authors.

4.2. Initiation of channel capture: The influence of chronology, basin size and river discharge reduction

In the previous section we elaborated on mechanisms sustaining and strengthening channel capture. The mechanism sustaining the present-day discharge partitioning is clear: the deeper Sibsa channel and the connecting channels more rapidly convey the tidal wave than the shallow Passur river, and therefore the Passur river is degenerating. It is also clear that both branches used to be more symmetric (before channel capture the Passur river was 15 m deeper than it used to be; Fig. 5) and that discharge portioning started with stronger amplification in the Sibsa than in the Passur. However, the mechanisms initiating this asymmetric amplification is open for interpretation.

Two hypotheses can be based on the order of land reclamations and the relative size of the basin. As conceptually illustrated in Fig. 12, the earlier construction of polders in the Sibsa would lead to tidal amplification also starting in the Sibsa (Fig. 4), thereby initiating channel capture. However, the Sibsa basin was not only reclaimed earlier but also more extensively (53–59 % in the Sibsa compared to 46 % in the Passur – Bain et al., 2019). Bain et al. did not explain how this difference in basin size reduction would lead to channel capture. Given the relationship between the reduction of intertidal areas and tidal amplification, it seems plausible that a larger reduction of its basin size led to larger amplification and increase in propagation speed in the Sibsa, which would then initiate the channel capture. Assuming that the impact of polder construction was much larger in the Sibsa than in the Passur, Fig. 4 may also be interpreted as follows. Polder construction led to tidal amplification and acceleration in the Sibsa, and only marginally in the Passur. The resulting cross-channel water level gradients drove an exchange flow between the Sibsa and the Passur, initiating erosion of the connecting rivers and channel capture. The moment the connecting channels were sufficiently large (in the early 1980's), the tidal range in the Passur began to amplify, driven by tidal dynamics of the Sibsa.

Bain et al. (2019) formulated two hypotheses to explain the capture of tidal prism by the Sibsa at the expense of the Passur, albeit not related to basin size. Their first hypothesis was based on observations by Pethick and Orford (2013) documenting the increase in tidal range in the Passur, and the assumption that tidal amplification had been less pronounced in the Sibsa. They then expanded on the work of Sassi et al. (2011) who observed that in tidally influenced river bifurcations with one long, shallow distributary and another short, deep distributary the river preferentially flows through the longer, shallow distributary where tidal propagation is more strongly dampened. Following Sassi's theory and assuming more tidal amplification in the Passur, this could lead to preferential more freshwater flow from the Gorai river via the upper Passur to the Sibsa. However, our data reveals that the tides in the Sibsa basin amplified as much as in the Passur.

A second alternative explanation of Bain et al. (2019) relates to the reduction in freshwater discharge into the Passur River (up to 50 % since the 1970's because of the construction of an upstream reservoir; Anwar et al., 2020). They hypothesize that before polder construction, the tidal wave entering the Passur river through the connecting channels was balanced by the larger river discharge at that time. A reduction in river discharge would then create an imbalance resulting in more tidal flow from the Sibsa to the Passur because they assumed the tidal wave celerity in the Sibsa to be slightly larger than that in the Passur at that moment in time. However, we believe that this mechanism requires a very large difference in wave celerity (because the Sibsa trajectory is longer) which would ultimately be the result of other aspects (such as polder construction, as elaborated above).

A final potential explanation is that the dimensions of the Sibsa river are such that the dominant tidal frequency is close to resonance. This makes the Sibsa system particularly vulnerable to human interventions. Talke and Jay (2020) identified two types of systems that are particularly prone to tidal amplification: systems that are shallow and strongly damping, in which a change in depth strongly influences the hydraulic drag, and systems that are close to resonance. The resonance length of a tidal basin is one quarter of the tidal wavelength (e.g. Pugh, 1987). For a depth of 10–15 m, which is typical for the Sibsa River (Fig. 5a), the tidal wavelength L given by $L = Tc$, with T the tidal period and c the speed of the tidal wave, is roughly 443–543 km when only accounting for the tidal channel (less when including the effect of the Sundarbans). The resonance length is therefore approximately 111–136 km. The Sibsa River terminates quite abruptly at 105 km from its mouth, where it

branches out over a number of shallow peripheral channels. This landward junction may act as a reflector of tidal energy, and the proximity of this terminus to the resonance length could be a reason that the Sibsa system responds more strongly to human interventions than the Passur. This could have initiated the asynchronous amplification of the tides and channel capture, as elaborated in more detail above.

The analysis of alternative mechanisms above suggests that channel capture is either the result of asynchronous polder development, or results from larger tidal amplification in the Sibsa, which in turn can be caused by either a larger reduction in basin size, or by tidal resonance. With the limited availability of field data, the exact underlying mechanism may never be ascertained. We can say, however, that flow capture is caused by asynchronous tidal amplification of two connected tidal basins in response to land reclamation, and that two positive feedback mechanisms exist which maintain and even strengthen the degeneration of both adjoining basins. The larger implications of such behaviour will be explored in more detail in the following section.

4.3. General implications for delta management

Understanding the feedback mechanisms described above are crucial for sustainable sediment management of the delta plain in Bangladesh. It is well known that polder construction led to shoaling of the blind peripheral channels which are in turn responsible for pluvial flooding and poor navigability of the local rivers. Local farmers therefore initiated so-called Tidal River Management (TRM) in 1990, a practice in which the embankments are cut to allow turbid water to settle in the polders, leading to higher bed levels within the polders and scouring of the blind peripheral channels. TRM became institutionalized since 1997, when the Bangladesh Water Development Board flooded a low-lying congested polder (Amir and Khan, 2019). Even though TRM has the potential to substantially reduce flood risks (Adnan et al., 2020) it is applied only limitedly. This is partly because of complex socio-economic issues but also because of the varying degree of success of TRM practice (Gain et al., 2017, Adnan et al., 2020). As elaborated in this study, the construction of polders not only initiated infilling of the blind peripheral channels, but also set in motion a complex response which not only led to poor polder drainage but also to shoaling of the Passur river channel, bank erosion, and tidal amplification. Shoaling of the Passur river adversely impacts navigability to the port of Mongla (the second-largest port of Bangladesh) requiring regular maintenance dredging. Bank erosion leads to large-scale loss of livelihood through erosion of houses and agricultural land (Fig. 13), and tidal amplification increases flood risks during storms. The adverse impact of polder construction is therefore larger than the issues it is usually associated with, such as pluvial flooding and shoaling of blind peripheral channels.

Solving these issues requires a holistic and nature-based water and sediment strategy, potentially including TRM, but possibly also measures aiming at more structurally restoring intertidal areas and closing of the connecting channels. Understanding the various feedback mechanisms is crucial for such an integral strategy, including appreciation of the long governing timescales. Polder construction started in the 1960's, but the tides were already amplified before polder construction (Fig. 3), probably caused by poorly embanked reclamations accommodating the increasing population inhabiting the delta plain of the Passur-Sibsa basin. Even after 50–60 years, the system still responds to this initial perturbation, and both bank erosion rates (Fig. 7) and tidal amplification rates (Fig. 3) are not slowing down. This period of response is long because of the large associated spatial scales, but also because of the positive feedback mechanisms resulting from the abundant sediment supply (preventing the system to attain morphological equilibrium).

These persistent, long-term responses also need to be accounted for within a larger context of climate-change and upstream changes in river runoff and sediment supply. The morphological concerns in the southwest of Bangladesh, including channel shoaling, bank erosion and pluvial flooding, are mainly caused by local human interventions in combination with the high sediment availability in the system. They are not, or only limitedly, caused by climate change or interventions in the upstream river basin. In the future, especially sea level rise will exacerbate existing problems of flooding and possibly erosion but at present, this is of secondary importance. However, although the high sediment availability is partly responsible for many of the present-day delta's environmental problems including flooding, bank erosion and channel degradation, it may also be part of the solution. Sediments strengthen the resilience of the GBD by allowing it to grow with SLR (Rogers and Overeem, 2017) through sediment deposition on the flood plains. Sedimentation rates in the Sundarbans exceed 1 cm/y (Rogers et al., 2013; Hale et al., 2019b) following human-induced tidal amplification (Bomer et al., 2020), suggesting sufficient sediment is available for the delta to keep pace with even larger rates of relative SLR.

Although the feedback mechanisms discussed in this paper have not yet been described in literature, we expect they play a role in more sediment-laden delta distributary networks around the world. Tidal amplification is commonly observed in many estuaries (e.g. Winterwerp and Wang, 2013; Talke and Jay, 2020) but in most of these estuaries human interventions take place simultaneously (e.g. Vellinga et al., 2014; van Maren et al., 2015, Zhu et al., 2019). We expect that tidal amplification in turbid estuarine systems in which large intertidal areas have been reclaimed results to a certain degree from the first positive feedback mechanism in Fig. 13. The absence of this feedback mechanism in scientific literature may result from lack of data (many large interventions took place before water level gauging stations were installed), simultaneous interventions (as explained above), or the fact that the Sibsa estuary is close to its resonance length and hence more sensitive to interventions.

To the authors' knowledge, the second mechanism schematized in Fig. 13 has been previously described only in the work of Bain et al. (2019). Similar to feedback mechanism 1, we believe this mechanism operates in many more deltas in the world. The stability of river bifurcations is a topic that has been extensively studied (see e.g. the review by Kleinhans et al., 2013), but the stability of their tidal counterpart is much less well investigated. Even in tidal environments the bifurcations that are well studied are tide-influenced but river-dominated, as in the Berau (Buschman et al., 2010), the Mahakam delta (Sassi et al., 2011), and the Kapuas (Kästner et al., 2017). Despite their fluvial dominance, these studies do demonstrate that tidal distributaries are more stable than fluvial distributaries (Hoitink et al., 2017). However, as both Fagherazzi (2008) and Hoitink et al. (2017) point out, these tidal channel networks are very sensitive to perturbations, which may potentially lead to a catastrophic channel reorganization. Large-scale land reclamation of intertidal areas is such a perturbation, especially when the intertidal areas of two parallel and connected tidal channels are not simultaneously reclaimed.

5. Conclusions

Analysis of the Passur-Sibsa tidal river network reveals that asynchronous or disparate reclaiming of intertidal areas has set in motion two feedback mechanisms. In the Sibsa River, where land reclamation at the expense of intertidal areas was larger but also started earlier, the loss of tidal storage led to amplification and faster propagation of the tides. Blind tidal channels at the landward side of the Sibsa have progressively filled up with sediment, leading to a continuing loss of tidal storage, reinforcing tidal amplification and propagation speed. This provides a first positive feedback loop in which tides amplify for a long period of time after the initial reclamation.

The increasing propagation speed in the Sibsa enabled it to capture tidal flow from the upper Passur tidal river through transverse, connecting channels. This river capture triggered a second positive feedback mechanism. First, the channel of the connecting channels and the Sibsa widened, further increasing the tidal penetration into the Passur River. Secondly, the tidal discharge through the initially more pristine Passur

distributary progressively reduced, resulting in channel shoaling, and therefore in a further reduction in tidal propagation speed. Both mechanisms strengthen the initial channel capture process, leading to expansion of the estuary that was developed first and degeneration of the more pristine distributary, even though the intertidal areas of the latter were reclaimed at a later stage as well.

This sequence of events started in the 1960's in the Sibsa estuary and still lead to large-scale channel infill, bank erosion, and tidal amplification. Satellite based expansion rates of rivers connecting the Passur and Sibsa Rivers that did not yet exist before polder construction, or were of minor importance, appear to be almost constant since 1988. A practical implication of this channel network reorganization is that polders cannot drain rainwater and suffer from pluvial flooding. Large scale bank erosion destroys agricultural land and houses, and waterways become unnavigable, including the navigation channel to Bangladesh's second-largest port. Interventions to solve these problems must account for these complex negative feedback mechanisms and provide integral, nature based holistic solutions.

Declaration of Competing Interest

The authors declare that they have no known competing financial interests or personal relationships that could have appeared to influence the work reported in this paper.

Data availability

The authors do not have permission to share data.

Acknowledgements

This work was funded by the Programme of Strategic Scientific Alliances between China and the Netherlands, the Zijiang Scholar Program of East China Normal University, a Deltares internal grant to support the NWO VICI program 'Deltas out of shape', and the 'Long Term Monitoring, Research and Analysis of Bangladesh Coastal Zone' project funded by the Bangladesh Water and Development Board. We acknowledge the great feedback provided by Steven Goodbred and an anonymous reviewer.

Appendix A. Supplementary material

Supplementary data to this article can be found online at https://doi.org/10.1016/j.catena.2022.106651.

References

Adnan, M.S.G., Haque, A., Hall, J.W., 2019. Have coastal embankments reduced flooding in Bangladesh? Sci. Total Environ. https://doi.org/10.1016/j.scitotenv.2019.05.048.
Adnan, M.S.G., Talchabhadel, R., Nakagawa, H., Hall, J.W., 2020. The potential of tidal river management for flood alleviation in south western Bangladesh. Sci. Total Environ. 731, 138747.
Amir, M.S.I.I., Khan, M.S.A., 2019. An innovative technique of Tidal River sediment management to solve the waterlogging problem in Southwestern Bangladesh. In: Coastal Management. Academic Press, pp. 165–199.
Anwar, M.S., Hasan, M.Z., Rahman, K., 2020. Salinity variation of south-western coastal region of Bangladesh in response to discharge from an upstream river. Int. J. Adv. Geosci. 8 (2), 173–178.
Auerbach, L.W., Goodbred Jr., S.L., Mondal, D.R., Wilson, C.A., Ahmed, K.R., Roy, K., et al., 2015. Flood risk of natural and embanked landscapes on the Ganges-Brahmaputra tidal delta plain. Nat. Clim. Chang. 5, 153–157.
Aziz, A., Paul, A.R., 2015. Bangladesh Sundarbans: present status of the environment and biota. Diversity 7, 242–269. https://doi.org/10.3390/d7030242.
Bain, R.L., Hale, R.P., Goodbred, S.L., 2019. Flow reorganization in an anthropogenically modified tidal channel network: an example from the southwestern Ganges-Brahmaputra-Meghna Delta. J. Geophys. Res. Earth Surf. 124, 2141–2159. https://doi.org/10.1029/2018JF004996.
Baptist, M.J., Babovic, V., Rodríguez Uthurburu, J., Keijzer, M., Uittenbogaard, R.E., Mynett, A., Verwey, A., 2007. On inducing equations for vegetation resistance. J. Hydraul. Res. 45 (4), 435–450. https://doi.org/10.1080/00221686.2007.9521778.
Bilskie, M.V., Hagen, S.C., Medeiros, S.C., Passeri, D.L., 2014. Dynamics of sea level rise and coastal flooding on a changing landscape. Geophys. Res. Lett. 41, 927–934.
Bomer, E.J., Wilson, C.A., Hale, R.P., Hossain, A.N.M., Rahman, F.M.A., 2020. Surface elevation and sedimentation dynamics in the Ganges-Brahmaputra tidal delta plain, Bangladesh: evidence for mangrove adaptation to human-induced tidal amplification. Volume 187. doi: 10.1016/j.catena.2019.104312.
Bricheno, L.M., Wolf, J., Islam, S., 2016. Tidal intrusion within a mega delta: an unstructured grid modelling approach. Estuar. Coast. Shelf Sci. 182 https://doi.org/10.1016/j.ecss.2016.09.014.
Brown, S., Nicholls, R.J., 2015. Subsidence and human influences in mega deltas: the case of the Ganges–Brahmaputra–Meghna. Sci. Total Environ. 527, 362–374. https://doi.org/10.1016/j.scitotenv.2015.04.124.
Buschman, F.A., Hoitink, A.J.F., van der Vegt, M., Hoekstra, P., 2010. Subtidal flow division at a shallow tidal junction. Water Resour. Res. 46, W12515. https://doi.org/10.1029/2010WR009266.
Chowdhury, M.R., 2000. An assessment of flood forecasting in Bangladesh: the experience of the 1998 flood. Nat. Hazards 22, 139–163. https://doi.org/10.1023/A:1008151023157.
Ericson, J.P., Vörösmarty, C.J., Dingman, S.L., Ward, L.G., Meybeck, M., 2006. Effective sea-level rise and deltas: causes of change and human dimension implications. Global Planet. Change 50 (1–2), 63–82.
Fagherazzi, S., 2008. Self-organization of tidal deltas. PNAS 105, 18692–18695.
Friedrichs, C.T., Aubrey, D.G., 1988. Non-linear tidal distortion in shallow well-mixed estuaries: a synthesis. Estuar. Coast. Shelf Sci. 27, 521–545.
Friedrichs, C.T., Aubrey, D.G., 1994. Tidal propagation in strongly convergent channels. J. Geophys. Res. 99, 3321e3336. https://doi.org/10.1029/93JC03219.
Gain, A.K., Benson, D., Rahman, R., Datta, D.K., Rouillard, J.J., 2017. Tidal river management in the south west Ganges-Brahmaputra delta in Bangladesh: moving towards a transdisciplinary approach? Environ. Sci. Policy 75, 111–120.
Giosan, L., Syvitski, J., Constantinescu, S., Day, J., 2014. Climate change: protect the world's deltas. Nat. News 516 (7529), 31.
Guo, L., van der Wegen, M., Jay, D.A., Matte, P., Wang, Z.B., Roelvink, D., He, Q., 2015. River-tide dynamics: exploration of nonstationary and nonlinear tidal behavior in the Yangtze River estuary. J. Geophys. Res. Oceans 120, 3499–3521. https://doi.org/10.1002/2014JC010491.
Hale, R.P., Wilson, C.A., Bomer, E.J., 2019a. Seasonal variability of forces controlling sedimentation in the Sundarbans National Forest, Bangladesh. Front. Earth Sci. 7, 211.
Hale, R.P., Bain, R., Goodbred Jr., S., Best, J., 2019b. Observations and scaling of tidal mass transport across the lower Ganges-Bramaputra delta plain: implications for delta management and sustainability. Earth Surf. Dynam. 7, 231–245. https://doi.org/10.5194/esurf-7-231-2019.
Hoitink, A.J.F., Wang, Z.B., Vermeulen, B., Huismans, Y., Kästner, K., 2017. Tidal controls on river delta morphology. Nat. Geosci. 10, 637–645. https://doi.org/10.1038/ngeo3000.
Hoitink, A.J.F., Nittrouer, J.A., Passalacqua, P., Shaw, J.B., Langendoen, E.J., Huismans, Y., van Maren, D.S., 2020. Resilience of river deltas in the Anthropocene. J. Geoph. Res.: Earth Surface 125 (3).
Hossain, N., 2018. The 1970 Bhola cyclone, nationalist politics, and the subsistence crisis contract in Bangladesh. Disasters 42 (1), 187–203. https://doi.org/10.1111/disa.12235.
Islam, T., Peterson, R.E., 2009. Climatology of landfalling tropical cyclones in Bangladesh 1877–2003. Nat. Hazards 48, 115–135. https://doi.org/10.1007/s11069-008-9252-4.
Iwantoro, A.P., Van Der Vegt, M., Kleinhans, M.G., 2020. Morphological evolution of bifurcations in tide-influenced deltas. Earth Surf. Dyn. 8 (2), 413–429.
IWM, 2003. Sundarban biodiversity conservation project, Surface water modelling. Final report, Volume 1, TA No. 3158-BAN, 137 p.
Jarriel, T., Isikdogan, L.F., Bovik, A., Passalacqua, P., 2020. System wide channel network analysis reveals hotspots of morphological change in anthropogenically modified regions of the Ganges Delta. Sci. Rep. 10 (1), 1–12.
Jian, J., Webster, P.J., Hoyos, C.D., 2009. Large-scale controls on Ganges and Brahmaputra river discharge on intraseasonal and seasonal time-scales. Q. J. R. Meteorol. Soc. 135, 353–370.
Kästner, K., Hoitink, A.J.F., Vermeulen, B., Geertsema, T.J., Ningsih, N.S., 2017. Distributary channels in the fluvial to tidal transition zone. J. Geophys. Res. Earth Surf. 122, 696–710. https://doi.org/10.1002/2016JF004075.
Kleinhans, M.G., Ferguson, R.I., Lane, S.N., Hardy, R.J., 2013. Splitting rivers at their seams: bifurcations and avulsion. Earth Surf. Proc. Land. 38 (1), 47–61.
Lentsch, N., Finotello, A., Paola, C., 2018. Reduction of deltaic channel mobility by tidal action under rising relative sea level. Geology 46, 599–602.
Lesser, G.R., Roelvink, J.A., Van Kester, J.A.T.M., Stelling, G.S., 2004. Development and validation of a three-dimensional morphological model. Coast. Eng. 51, 883–915.
Li, C., Schuttelaars, H.M., Roos, P.C., Damveld, J.H., Gong, W., Hulscher, S.J.M.H., 2016. Influence of retention basins on tidal dynamics in estuaries: application to the Ems estuary. Ocean Coast. Manag. 134, 216–225. https://doi.org/10.1016/j.ocecoaman.2016.10.010.
NEDECO, 1967. East Pakistan inland water transport authority: surveys of inland waterways and ports 1963–1967 (Vol. 3, hydrology and morphology).
Nicholls, R.J., Cazenave, A., 2010. Sea-level rise and its impact on coastal zones. Science 328, 1517–1520.
Nienhuis, J.H., Ashton, A.D., Edmonds, D.A., Hoitink, A.J.F., Kettner, A.J., Rowland, J.C., Törnqvist, T.E., 2020. Global-scale human impact on delta morphology has led to net land area gain. Nature 577 (7791), 514–518.

Nishat, B., Zobaidur Rahman, A.J.M., Mahmud, S., 2019. Landscape narrative of the Sundarban: towards collaborative management by Bangladesh and India. IWM Report Prepared for the World Bank.

Passalacqua, P., Giosan, L., Goodbred, S., Overeem, I., 2021. Stable ≠ sustainable: Delta dynamics versus the human need for stability. Earth's Fut. 9, e2021EF002121 https://doi.org/10.1029/2021EF002121.

Paszkowski, A., Goodbred, S., Borgomeo, E., Khan, M., Hall, J.W., 2021. Geomorphic change in the Ganges–Brahmaputra–Meghna delta. Nat. Rev. Earth Environ. 2 (11), 763–780.

Pawlowicz, R., Beardsley, B., Lentz, S., 2002. Classical tidal harmonic analysis including error estimates in MATLAB using T_TIDE. Comput. Geosci. 28, 929–937.

Pethick, J., Orford, J.D., 2013. Rapid rise in effective sea-level in southwest Bangladesh: its causes and contemporary rates. Global Planet. Change 111, 237–245. https://doi.org/10.1016/j.gloplacha.2013.09.019.

Pugh, D.T., 1987. Tides, Surges, and Mean Sea Level. John Wiley and Sons Ltd, Chichester.

Rahman, M., 2017. Study on morphological change and navigation problems of Passur River in Bangladesh. Khulna University of Engineering and Technology. Master's thesis.

Rahman, M., Dustegir, M., Karim, R., Haque, A., Nicholls, R.J., Darby, S.E., Nakagawa, H., Hossain, M., Dunn, F.E., Akter, M., 2018. Recent sediment flux to the Ganges-Brahmaputra-Meghna delta system. Sci. Total Environ. 643, 1054–1064. https://doi.org/10.1016/j.scitotenv.2018.06.147.

Rahman, M., Ali, Md., 2018. Potential causes of navigation problem in Passur river and interventions for navigation enhancement. In: Proceedings of the 4th International Conference on Civil Engineering for Sustainable Development (ICCESD-2018), 9–11 February 2018, KUET, Khulna, Bangladesh (ISBN-978-984-34-3502-6).

Renaud, F.G., Syvitski, J.P., Sebesvari, Z., Werners, S.E., Kremer, H., Kuenzer, C., Friedrich, J., 2013. Tipping from the Holocene to the Anthropocene: How threatened are major world deltas? Curr. Opin. Environ. Sustain. 5 (6), 644–654.

Rogers, K.G., Overeem, I., 2017. Doomed to drown? Sediment dynamics in the human-controlled floodplains of the active Bengal Delta. Elem. Sci. Anth. 5, 66. https://doi.org/10.1525/elementa.250.

Rogers, K.G., Goodbred, S.L., Mondal, D.R., 2013. Monsoon sedimentation on the "abandoned" tide-influenced Ganges-Brahmaputra delta plain. Estuar. Coast. Shelf Sci. 131, 297–309.

Sassi, M.G., Hoitink, A.J.F., 2013. River flow controls on tides and tide-mean water level profiles in a tidal freshwater river. J. Geophys. Res. Oceans 118 (9), 4139–4151.

Sassi, M.G., Hoitink, A.J.F., de Brye, B., Vermeulen, B., Deleersnijder, E., 2011. Tidal impact on the division of river discharge over distributary channels in the Mahakam Delta. Ocean Dyn. 61, 2211–2228. https://doi.org/10.1007/s10236-011-0473-9.

Shaha, D.C., Cho, Y.K., 2016. Salt plug formation caused by decreased river discharge in a multi-channel estuary. Sci. Rep. 6, 27176. https://doi.org/10.1038/srep27176.

Song, D., Wang, X.H., Zhu, X., Bao, X., 2013. Modeling studies of the far-field effects of tidal flat reclamation on tidal dynamics in the East China Seas. Estuar. Coast. Shelf Sci. 133, 147–160.

Stark, J., Smolders, S., Meire, P., Temmerman, S., 2017. Impact of intertidal area characteristics on estuarine tidal hydrodynamics: a modelling study for the Scheldt Estuary. Estuar. Coast. Shelf Sci. 198, 138–155.

Syvitski, J.P.M., Vörösmarty, C.V., Kettner, A.J., Green, P., 2005. Impact of humans on the flux of terrestrial sediment to the global coastal ocean. Science 308, 376–380.

Syvitski, J.P.M., Kettner, A.J., Overeem, I., Hutton, E.W.H., HannonMT, B.GR., 2009. Sinking deltas due to human activities. Nat. Geosci. 2, 681–686.

Talke, S.A., Jay, D.A., 2020. Changing tides: the role of natural and anthropogenic factors. Ann. Rev. Mar. Sci. 12, 121–151.

Tessler, Z.D., Vörösmarty, C.J., Grossberg, M., Gladkova, I., Aizenman, H., Syvitski, J.P., Foufoula-Georgiou, E., 2015. Profiling risk and sustainability in coastal deltas of the world. Science 349, 638–643. https://doi.org/10.1126/science.aab3574.

van Maren, D.S., van Kessel, T., Cronin, K., Sittoni, L., 2015. The impact of channel deepening and dredging on estuarine sediment concentration. Cont. Shelf Res. 95, 1–14. https://doi.org/10.1016/j.csr.2014.12.010.

Vellinga, N.E., Hoitink, A.J.F., van der Vegt, M., Zhang, W., Hoekstra, P., 2014. Human impacts on tides overwhelm the effect of sea level rise on extreme water levels in the Rhine-Meuse delta. Coast. Eng. 90, 40–50.

Vörösmarty, C.V., Meybeck, M., Fekete, B., Sharma, K., Green, P., Syvitski, J., 2003. Anthropogenic sediment retention: major global impact from registered river impoundments. Global Planet. Change 39, 169–190.

Wilson, C., Goodbred, S., Small, C., Gilligan, J., Sams, S., Mallick, B., Hale, R., 2017. Widespread infilling of tidal channels and navigable waterways in human-modified tidal deltaplain of southwest Bangladesh. Elementa 5, 78. https://doi.org/10.1525/elementa.263.

Winterwerp, J.C., Wang, Z.B., 2013. Man-induced regime shifts in small estuaries – I: theory. Ocean Dyn. 63 (11–12), 1279–1292.

Wright, L.D., Coleman, J.M., 1973. Variations in morphology of major river deltas as functions of ocean wave and river discharge regimes. Am. Assoc. Pet. Geol. Bull. 57, 370–398.

Zhu, C., Guo, L., van Maren, D.S., Tian, B., Wang, X., He, Q., Wang, Z.B., 2019. Decadal morphological evolution of the mouth zone of the Yangtze estuary in response to human interventions. Earth Surf. Proc. Land. 44 (12), 2319–2332. https://doi.org/10.1002/esp.4647.